Partial Photoionization Cross Sections and Angular Distributions for Double Excitation of Helium up to the $N = 13$ Threshold

A. Czasch,[1,*] M. Schöffler,[1] M. Hattass,[1] S. Schössler,[1] T. Jahnke,[1] Th. Weber,[1] A. Staudte,[1] J. Titze,[1] C. Wimmer,[1] S. Kammer,[1] M. Weckenbrock,[1] S. Voss,[1] R. E. Grisenti,[1] O. Jagutzki,[1] L. Ph. H. Schmidt,[1] H. Schmidt-Böcking,[1] R. Dörner,[1] J. M. Rost,[2] T. Schneider,[2] Chien-Nan Liu,[3] I. Bray,[4] A. S. Kheifets,[5] and K. Bartschat[6]

[1]*Institut für Kernphysik, Universität Frankfurt, D-60438 Frankfurt, Germany*
[2]*Max-Planck-Institut für Physik komplexer Systeme, D-01187 Dresden, Germany*
[3]*Fu Jen Catholic University, Taipei, Taiwan*
[4]*Murdoch University, Perth, Western Australia 6150, Australia*
[5]*Australian National University, Canberra ACT 0200, Australia*
[6]*Drake University, Des Moines, Iowa 50311, USA*

(Received 1 November 2004; published 8 December 2005)

Partial photoionization cross sections $\sigma_N(E_\gamma)$ and photoelectron angular distributions $\beta_N(E_\gamma)$ were measured for the final ionic states $He^+(N > 4)$ in the region between the $N = 8$ and $N = 13$ thresholds ($E_\gamma > 78.155$ eV) using the cold target recoil ion momentum spectroscopy technique (COLTRIMS). Comparison of the experimental data with two independent sets of theoretical predictions reveals disagreement for the branching ratios to the various He_N^+ states. The angular distributions just below the double ionization threshold suggest an excitation process for highly excited N states similar to the Wannier mechanism for double ionization.

DOI: 10.1103/PhysRevLett.95.243003 PACS numbers: 32.80.Dz, 32.80.Fb

In quantum theory helium has always been considered as the archetypical counterpart of the classical three-body system. In 1963 Madden and Codling [1] investigated the double excitation of helium into $^1P^0$ states using synchrotron radiation. These measurements initiated a continuous sequence of theoretical [2–9] and experimental [10–14] work. Doubly excited states become visible as resonances in the photon energy dependence of the single ionization cross section. These resonances are organized in series converging towards the thresholds I_N of the hydrogenlike final ionic $He^+(N)$ states. The most commonly used classification scheme [2,3] consists of five approximate quantum numbers $N(K, T)_n^A$, which unambiguously denote doubly excited states. Above $I_{N=4}$ members of higher lying series interfere with lower series and act as so-called perturbers [9,10]. Above $I_{N=8}$ ($E_\gamma > 78.155$ eV) the interaction between different series renders the identification of individual resonances impossible because the line widths exceed the average spacing between the resonances. In this regime the $N(K, T)_n^A$ classification scheme is expected to break down, raising the question whether evidence for quantum chaos [15], manifested in Ericson fluctuations, exists in helium. Recently, numerical results above $I_{N=8}$ were analyzed using nearest neighbor spacing statistics [14]. This analysis revealed a tendency towards a Wigner distribution, which may be an indication for quantum chaos.

Here we report a measurement of partial cross sections and angular distributions, as a continuous function of energy, in the region close to the double ionization threshold at 79.0052 eV. The partial cross sections reveal significant disagreement (up to a factor of 2) compared to theory. The measured angular distributions converge towards $\beta = -1$ for highly excited states N. This behavior was already predicted by Greene [8] 25 years ago. As discussed below, the angular distributions might be interpreted using an analogy to the Wannier escape mechanism for double ionization, although excitation-ionization is not part of the original Wannier theory.

Historically the double excitation of helium by photon absorption was investigated using a variety of different techniques. Originally [1] the total photon absorption cross section was measured as a function of the photon energy. During recent decades, however, gas cell measurements of the total He^+ ionization yield as a function of the photon energy were most common [10,13]. In a recent measurement [14] a photon energy of $E_\gamma = 78.33$ eV, i.e., between the $I_{N=8}$ and $I_{N=9}$ thresholds, was reached. To date this is the only experimental data in the interesting regime close to the double ionization threshold.

A far more powerful technique for the investigation of autoionizing doubly excited states is electron spectroscopy. Measuring the kinetic energies of the photoelectrons allows for the separation of the final states of the residual $He^+(N)$ ion. The measured angular distribution of the emitted photoelectrons is sensitive to the distribution of the contributing angular momenta ℓ. As shown in Ref. [12] the resonances of fairly weak series may be visible as pronounced fluctuations in the angular distributions. The authors reported partial cross sections of photoelectron emission $\sigma_N(E_\gamma)$ and angular distributions $\beta_N(E_\gamma)$ for $He^+(N \leq 5)$. In a more recent publication [11] partial cross sections were reported up to the $He^+(N = 5)$ threshold, but no angular distributions were shown.

With the recent growth of computing power the interesting regime above $N = 8$ has become accessible for theorists [6,7]. However, experimental research in this energy region remains an extremely demanding task due to very low partial cross sections. Both techniques—measurements of the total cross section on one side and electron spectroscopy on the other—suffer from this fact in different ways. Measuring total cross sections relies on the detection of small fluctuations in the presence of a huge background signal [10] mostly consisting of $He^+(N = 1, 2)$ states. Electron spectrometry, on the other hand, seems well suited to solve these problems since it allows for the separation of different final states $He^+(N)$. However, the small angular acceptance of traditional electron spectrometers reduces the detection efficiency of these systems dramatically. In order to overcome these obstacles we applied the COLTRIMS imaging technique [16,17] to the problem. Among the most striking advantages of these spectrometers is an angular acceptance of 4π combined with multiparticle detection. Two time and position sensitive multichannel plate detectors [18] ($Ø = 80$ mm) combined with delayline anodes for position readout are located vis-à-vis around the reaction zone. The photon beam intersects a narrow and cold supersonic helium gas jet (density 10^{12} cm^{-2}) which defines the geometry of the reaction zone. A weak homogenous electrostatic field (2 V/cm) guides the emitted particles towards the detectors. Thus electrons and He^+ ions can be detected in coincidence. Since the fields inside the spectrometer are known, the reconstruction of the initial momenta is straightforward. The measurement was performed at the beam line U125/1-PGM at the German synchrotron facility BESSY II. At the beginning and at the end of the beam time the degree of polarization ($1.0 \pm 1.8 \times 10^{-3}$) and the photon energy resolution of $\Delta E_\gamma = 3.9$ meV FWHM were determined. ΔE_γ was derived by scanning the $2, 1_4$ resonance at $E_\gamma = 64.136$ eV and comparing the result with experimental and theoretical values in the literature (e.g., Ref. [13]). The degree of linear polarization was determined by measuring the angular distribution of electrons emitted 0.5 eV above the single ionization threshold. The absolute energy of the monochromator was calibrated by locating the $2, 1_4$ resonance and the various thresholds for $He^+(N > 8)$ using the formula $E_N = 79.0052$ eV $- 13.6$ eV $Z^2 N^{-2}$. The achieved absolute photon energy calibration is better than ± 2.0 meV. The acquired data set covers the photon energy region between $E_\gamma = 78.155$ eV [threshold for $He^+(N = 8)$] and $E_\gamma = 78.88$ eV. A stepsize of 3 meV and a photon energy resolution of $\Delta E_\gamma = 3.9$ meV FWHM was chosen for the scan. Between 78.48 and 78.792 eV the scan was performed with higher speed and less statistics per data point, hence leading to larger error bars in this region. Final states up to $N = 13$ could be clearly identified (Fig. 1).

Figure 1(a) shows the kinetic energies of the emitted electrons in the photon energy range above $E_\gamma > 78.155$ eV. The different lines can be assigned to the various final states of the residual $He^+(N)$ ion. The intensity of these lines encodes the count rate of the corresponding autoionization channel. The intensities are shown in Fig. 1(b) where the branching ratios (in %) between different reaction channels $He^+(N)$ and the total cross section for He^+ are displayed. The discussion below focuses on the region below 78.48 eV, where the scan was performed in a slower mode in order to determine data points with an appropriate statistical accuracy. The statistical error bars in this region are negligibly small. The most obvious fea-

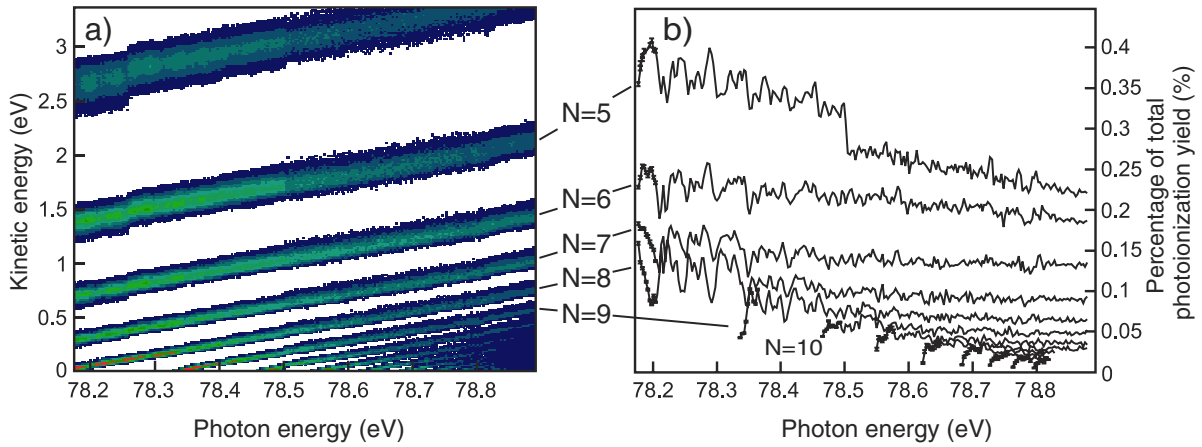

FIG. 1 (color online). (a) The kinetic energies of the emitted photoelectrons displayed as function of the photon energy. The lines can be assigned to different hydrogenlike finals states of the residual $He^+(N)$ ion with N denoting the principal quantum number. (b) The relative partial cross sections $\sigma_N(E_\gamma)$. The steplike structure in $\sigma_{N=5}$ is a technical artifact. [The curve should be shifted up for $E > 78.5$ eV]. The data was normalized by dividing the count rate of the various channels by the total number of detected He^+ ions. This method ensures that fluctuations in the absolute count rate, possibly caused by a varying target density or photon flux, do not affect the results.

ture is the similarity between different curves. Structures visible in curve N are also visible in curve $N-1$. Additionally, a slight horizontal shift between different curves is visualized by a tilted dashed line in Fig. 2. This shift, whose origin is unknown, is about 7 meV between $N=5$ and $N=8$. This feature is well reproduced in both calculations we compare with. Since neither model includes relativistic effects or accounts for the finite mass of the nucleus, these factors can not cause the shift.

We compare the data to calculations [7] based on the eigenchannel R-Matrix method [19] using a close-coupling scheme [20] and to calculations applying the convergent close-coupling (CCC) approach [21]. In these models the photon is absorbed by one of the He electrons, and then the problem essentially becomes electron scattering from the He^+ ion with the proper asymptotic boundary condition for ionization processes [22]. A highly accurate description of the correlated He ground state is important to produce essentially gauge-independent results [21]. The CCC cross sections in the length, velocity, and acceleration gauges differ by less than 10%. Recently, the original Laguerre-based CCC method was modified to allow for the use of a box basis, which discretizes the target spectrum by forcing all target wave functions to vanish at the box boundary R_0 [23]. This approach is particularly attractive here because it readily allows for the generation of large-N eigenstates by simply increasing R_0. Taking $R_0 = 600$ a.u. we generated $15-\ell$ negative-energy states, of which $13-\ell$ are good eigenstates. Since the inclusion of positive-energy states was also important, we used $22-\ell$ states for each orbital angular momentum $\ell \leq 5$, leading to a total of 117 states. The CCC calculations were performed separately for each energy at a spacing of 2 meV. Thus resonances with a width smaller than 2 meV may not have been sufficiently resolved.

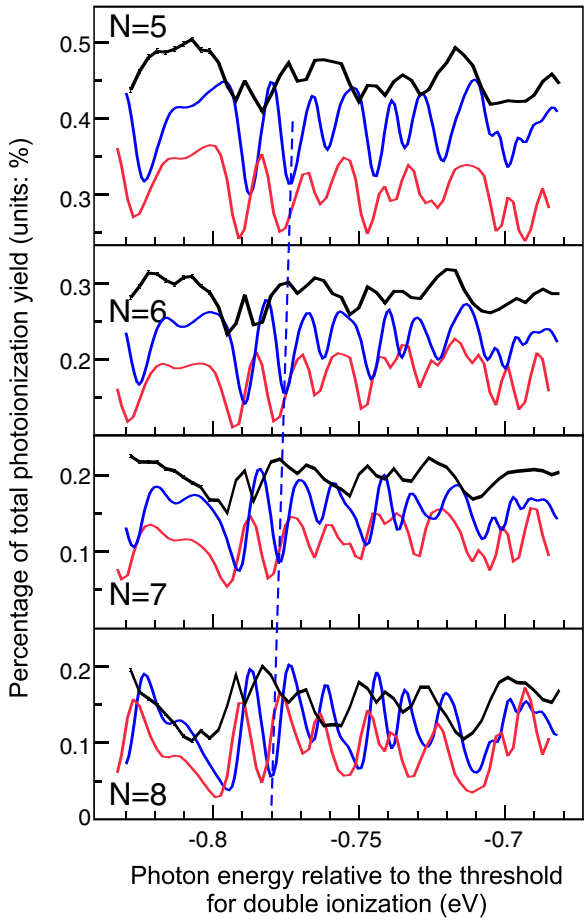

FIG. 2 (color online). Comparison between experiment (black) and theory. The blue (dark gray) and the red (light gray) curves are results from R-matrix [7] and CCC calculations (both in the velocity gauge). The statistical errors in each black curve are very small (about twice the line width). However, there might be a systematic error (less than 10%) that could reduce the measured cross sections as a whole. The theoretical data were convoluted with a Gaussian distribution of 3.9 meV FWHM. The energy scale is shown relative to the respective experimental or theoretical double ionization thresholds (Experiment: 79.0052 eV, R matrix: 79.006 eV, CCC: 79.0089 eV). The overall mismatch between the curves is 4.5 meV (CCC-experiment) and 7.0 meV (R matrix-experiment). A general shift between the curves is indicated by a tilted dashed line.

In Fig. 2 the measured cross sections (branching ratios) are compared to both independent state-of-the-art calculations. These nonrelativistic theories do not account for the finite mass of the nucleus, and thus the absolute ground state energy (i.e., the double ionization threshold) differs from experiment by up to 10 meV. In order to compare all three data sets on a common energy scale, we plotted the curves relative to their respective threshold of double ionization. Almost all peaks found in the experiment are reproduced in both calculations. However, the absolute position is shifted by up to 7 meV, and there is clear disagreement in the average values of the branching ratios. The theories disagree among each other by up to a factor of 1.5. A similar disagreement between measurement and theory was reported at lower photon energies $E_\gamma < 76.8$ eV for $N \leq 6$ [11]. As in the present case, the measured cross sections [11] were larger than predicted by theory. However, in a previous experiment Menzel *et al.* [12] found good agreement between their experimental data and calculations for $N \leq 4$.

We now turn to the next level of detail. The β-parameter characterizing the angular distribution exhibits a similar wealth of structure as the partial cross sections [Fig. 3(a)]. From these complex patterns one might expect a breakdown of the $N(K,T)^A_N$ scheme. However, this is misleading. Despite these overlapping resonances, the underlying excitation and decay dynamics is quite intuitive and seems to be valid when passing through the double ionization threshold. The onset values of β_N at their respective thresholds converge towards -1 as the double ionization threshold is approached from below [Fig. 3(b)]. This was predicted by Greene [8] [based on Herricks SO(4) classi-

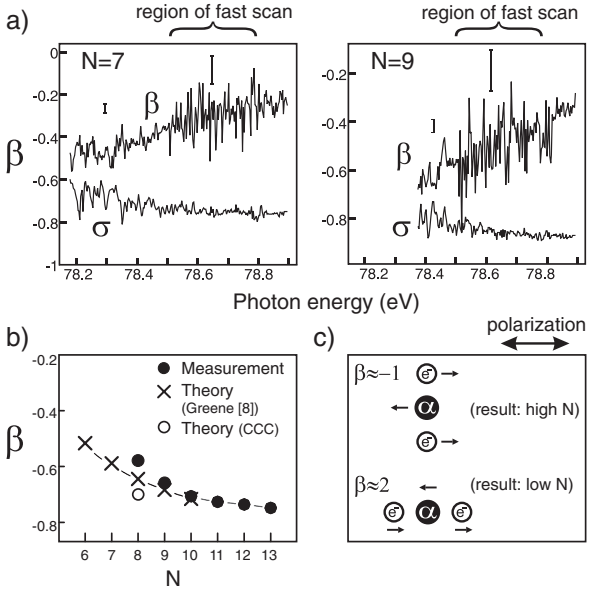

FIG. 3. (a) The angular distributions (β parameter) of photoelectrons from different channels as a function of the photon energy. The partial cross sections σ_N, displayed in arbitrary units, demonstrate the correlation between both curves. This correlation is a known feature which was also observed at lower energies [12]. Because of space limitations other measured β parameters for $N = 5, 6, 8, 10$ are not shown. The larger error bars are assigned to the middle part of the scan where less statistics was acquired ($78.48\ \text{eV} < E_\gamma < 78.792\ \text{eV}$). (b) Comparison with two calculations at the corresponding threshold for each final state N. The experimental error bars are of the same size as the circles. (c) The ionization and excitation into high N states depends on the orientation of the e-α-e system relative to the polarization vector. Highly excited final states are populated preferably in conjunction with $\beta \approx -1$.

fication]. It joins smoothly with the situation just above threshold, where the Wannier law and experiment show a similar behavior [24]. In this picture the metastable e-α-e configuration, where the nucleus resides on the potential saddle between the two electrons, plays a key role [Fig. 3(c)]. The preferred way to populate such a state is by absorption of a linearly polarized photon. If the configuration is oriented perpendicular to the polarization vector, the electric field of the photon can drive the system along the stable direction of the saddle. Thus the electrons must be aligned perpendicular to the field vector (corresponding to $\beta = -1$) and the nucleus is moved parallel to the polarization vector. Above the threshold for double ionization, this motion of the nucleus can be seen directly [24]. The other configuration, where the e-α-e system is oriented parallel to the electric field, results in the capture of one of the electrons in a more deeply bound state and hence does not contribute to states with high N.

In conclusion: the problem of double excitation of the simplest two-electron system very close to the threshold for double ionization still poses a major challenge to theory and experiment. The angular distributions of near zero kinetic energy electrons indicate an excitation mechanism, which can be understood by Wannier-type stability considerations when passing through the threshold for double ionization.

The experimental work was supported by the DFG and BMBF (Internationales Büro). We thank the German synchrotron facilities HASYLAB and BESSY II for financial support and beam time, and Drs. Reichardt, Follath, and Möller for excellent support during the beam times. A. S. thanks the Studienstiftung des deutschen Volkes for support. A. C. and Th. W. thank the Graduiertenförderung des Landes Hessen for support. I. B. and A. S. K acknowledge support from the Australian Research Council, and K. B. acknowledges support from the National Science Foundation (USA).

*Electronic address: czasch@atom.uni-frankfurt.de

[1] R. P. Madden and K. Codling, Phys. Rev. Lett. **10**, 516 (1963).
[2] D. R. Herrick and O. Sinanŏglu, Phys. Rev. A **11**, 97 (1975).
[3] C. D. Lin, Phys. Rev. Lett. **51**, 1348 (1983); Phys. Rev. A **29**, 1019 (1984).
[4] J. M. Feagin and J. S. Briggs, Phys. Rev. Lett. **57**, 984 (1986); Phys. Rev. A **37**, 4599 (1988).
[5] G. Tanner, K. Richter, and J. M. Rost, Rev. Mod. Phys. **72**, 497 (2000).
[6] H. W. van der Hart and C. H. Greene, Phys. Rev. A **66**, 022710 (2002).
[7] T. Schneider, C.-N. Liu, and J. M. Rost, Phys. Rev. A **65**, 042715 (2002).
[8] C. H. Greene, Phys. Rev. Lett. **44**, 869 (1980).
[9] J. M. Rost, K. Schulz, M. Domke, and G. Kaindl, J. Phys. B **30**, 4663 (1997).
[10] M. Domke *et al.*, Phys. Rev. A **53**, 1424 (1996).
[11] Y. H. Jiang *et al.*, Phys. Rev. A **69**, 042706 (2004).
[12] A. Menzel *et al.*, Phys. Rev. Lett. **75**, 1479 (1995); Phys. Rev. A **54**, 2080 (1996).
[13] K. Schulz *et al.*, Phys. Rev. Lett. **77**, 3086 (1996).
[14] R. Püttner *et al.*, Phys. Rev. Lett. **86**, 3747 (2001).
[15] J.-P. Connerade, J. Phys. B **30**, L31 (1997).
[16] R. Dörner *et al.*, Phys. Rep. **330**, 95 (2000).
[17] J. Ullrich *et al.*, Rep. Prog. Phys. **66**, 1463 (2003).
[18] http://www.roentdek.com.
[19] P. F. O'Mahony and C. H. Greene, Phys. Rev. A **31**, 250 (1985).
[20] C. Pan, A. F. Starace, and C. H. Greene, Phys. Rev. A **53**, 840 (1996).
[21] A. S. Kheifets and I. Bray, Phys. Rev. A **57**, 2590 (1998).
[22] R. J. W. Henry and L. Lipsky, Phys. Rev. **153**, 51 (1967).
[23] I. Bray, K. Bartschat, and A. T. Stelbovics, Phys. Rev. A **67**, 060704(R) (2003).
[24] R. Dörner *et al.*, Phys. Rev. Lett. **77**, 1024 (1996).